Topological transition and its connection with the conductivity and thermopower anomalies in two-dimensional systems

N. N. Ablyazov, M. Yu. Kuchiev, and M. E. Raikh
A. F. Ioffe Physico Technical Institute, Leningrad 194 021, U.S.S.R.
and Physik Department E-16, Technische Universität München, D-8046 Garching, Federal Republic of Germany

(Received 3 December 1990; revised manuscript received 11 June 1991)

The conductivity and thermopower of a two-dimensional electron gas in the case when the Fermi level is placed near the origin of one of the size-quantization subbands are considered. The intersection of the Fermi level with the size-quantization level causes the topological change of the Fermi surface, which results in anomalies in the conductivity and thermopower. It is shown that a consistent quantitative description of the anomaly requires that the distortion of the electronic states in the populating subband by the random potential be taken into account. A general expression for the electron relaxation time in the vicinity of the transition is derived with the use of diagrammatic techniques. Detailed calculations are performed for two models of the random potential: Gaussian white noise and the screened Coulomb potential.

I. INTRODUCTION

It is well known that in two-dimensional (2D) semiconductor systems, such as quantum wells, metal-oxide-semiconductor (MOS) structures, and δ-doping layers, the electronic states represent the set of the size-quantization subbands. The corresponding dispersion law for the ith subband reads

$$\varepsilon_i(k)=E_i+\frac{\hbar^2k^2}{2m}\ , \tag{1}$$

where E_i is the position of the quantized energy level in the z direction, $\mathbf{k}$ is the wave vector in the xy plane, and m is the electron mass.

The position of the Fermi level at zero temperature is determined by the doping or by the gate voltage. For certain parameters of the structure by tuning the gate voltage the continuous transition from the case $E_F<E_i$ to the case $E_F>E_i$ can be traced (see, for example, the experimental papers of Refs. 1 and 2). Figure 1 illustrates such a transition for $i=2$. It is seen that at the threshold

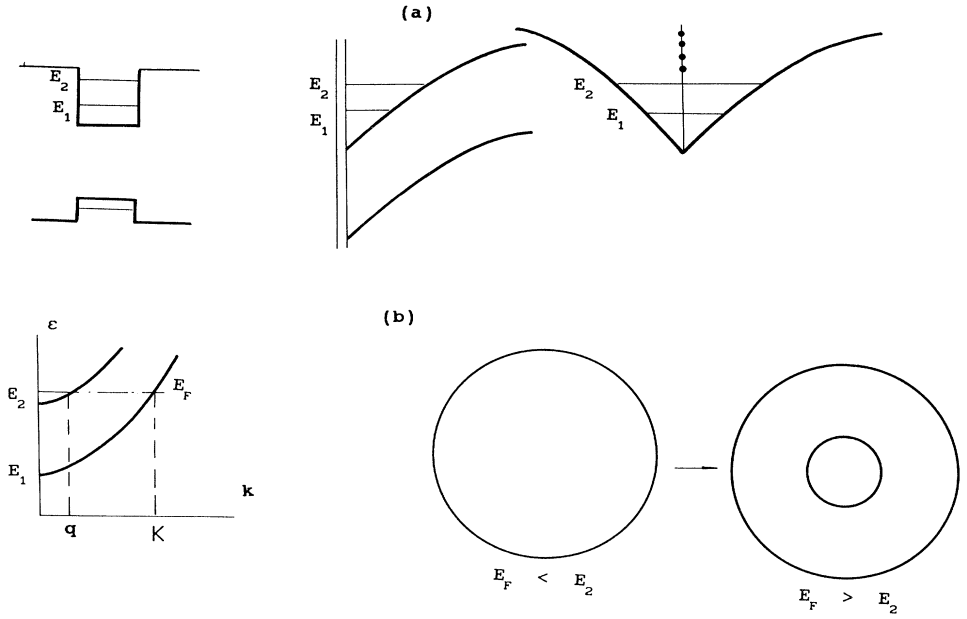

FIG. 1. (a) The examples of 2D semiconductor structures: quantum well, MOS structure, and δ-doping layer with the quantized spectrum of the transverse motion. (b) The dispersion law for the first two subbands and the transformation of the Fermi surface in the vicinity of the transition.

of transition ($E_F=E_2$) the Fermi surface changes its topology. It is a circle for $E_F<E_2$ becoming a pair of circles for $E_F>E_2$.

The peculiarities of the thermodynamic characteristics (such as specific heat and magnetic susceptibility) of bulk metal caused by the change of the Fermi surface topology were first considered by Lifshitz.[3] In a number of recent works, Varlamov and Pantsulaya[4–6] consider the kinetic properties of the bulk metal in the vicinity of topological transition. It was shown that conductivity and thermopower as the function of the Fermi level exhibit anomalous behavior.

The 2D case considered in this paper has an advantage of more pronounced anomalies. The basis for this is a staircase behavior of the density of states in the 2D case. The newly created part of the Fermi surface corresponding to the population of the next subband has a finite density of states just after creation. As a result the conductivity exhibits sharp, steplike decrease at the threshold of transition. This fact was discussed in Refs. 7 and 8 in the framework of the Boltzmann equation. The result obtained predicts the discontinuity of the conductivity at the threshold and, hence, the divergency of the thermopower. However it is clear that in real systems the discontinuities should be rounded. Therefore the more sophisticated consideration of the transition is needed.

An attempt to work out the improved description of the conductivity anomaly was undertaken by Cantrell and Butcher.[9] Their approach is similar to that used by Varlamov and Pantsulaya in the 3D case. As we shall demonstrate later, in the 2D case such an approach proves not to be sufficient. The neglected terms appear to be of the same order as those taken into account.

The main purpose of this paper is to demonstrate that in the vicinity of the topological transition the problem can be solved exactly. The quantitative description of the behavior of the conductivity and thermopower is given.

The paper is arranged in the following way. In Sec. II the general relation reducing the calculation of conductivity and thermopower to the calculation of the self-energy of the electron in a random potential is derived. The evaluation of the self-energy with the use of the diagram method is carried out in Sec. III. In Sec. IV the results of the calculation of the conductivity and thermopower for two models of random potential is presented. The experimental consequences of the theory are discussed in Sec. IV.

II. GENERAL RELATIONS

We restrict our consideration to the case when only the two lowest subbands give the contribution to the conductivity. The dispersion curves for the electrons in these subbands are shown if Fig. 1. The Fermi level is placed close to E_2. We consider the low-temperature limit when the electron mobility is limited by the elastic scattering by a random potential. The random potential usually originates from charged donors located in the spacer layer, impurities in the conducting channel, surface roughness, alloy fluctuations, etc.

It is seen from Fig. 1 that the electron from the first subband can be elastically scattered into the second subband and vice versa. The effect of these intersubband scattering processes on the conductivity σ was studied by Mori and Ando[8] (see also Ref. 10). The result obtained reads

$$\sigma=\sigma_1+\sigma_2=e(n_1\mu_1+n_2\mu_2)\ , \tag{2}$$

where σ_1, n_1 and σ_2, n_2 are the partial conductivity and electron concentration for subbands 1 and 2. The usual relation

$$\mu_i=\frac{e\tau_i}{m} \tag{3}$$

between the mobility μ_i and the relaxation time τ_i is supposed. Note that intersubband scattering influences both τ_1 and τ_2. According to Ref. 8 these quantities are to be found from the system of equations

$$S_{11}\tau_1+S_{12}\tau_2=1,\quad S_{12}\tau_1+S_{22}\tau_2=1\ , \tag{4}$$

where

$$S_{ij}=\frac{2\pi\hbar^2}{m}\int\frac{d^2k}{(2\pi)^2}\delta(\varepsilon_1(\mathbf{k})-E_F)\times\left[\sum_{\mathbf{k}'}\left[\delta_{ij}\sum_{l=1,2}W^{(i,l)}_{\mathbf{k},\mathbf{k}'}-W^{(i,j)}_{\mathbf{k},\mathbf{k}'}\frac{\mathbf{k}\cdot\mathbf{k}'}{k^2}\right]\right]\ , \tag{5}$$

$$W^{(i,l)}_{\mathbf{k},\mathbf{k}'}=\frac{2\pi}{\hbar}\langle|(i,\mathbf{k}|V(\mathbf{r})|l,\mathbf{k}')|\rangle^2\delta(E_F-\varepsilon_l(\mathbf{k}'))\ . \tag{6}$$

Here $V(\mathbf{r})$ is a random potential. The symbol $\langle\ \rangle$ denotes the configurational averaging. The stages $|i,\mathbf{k})$ are

$$|i,\mathbf{k})=\frac{1}{\Omega^{1/2}}\Psi_i(z)\exp(i\mathbf{k}\cdot\boldsymbol{\rho})\ , \tag{7}$$

where $\Psi_i(z)$ is the normalized wave function describing the transverse movement. The corresponding size-quantization energy is E_i; Ω is the normalization area.

The terms with $i=j=1$ in Eq. (5) describe the intrasubband scattering. They give the standard formula for the inverse transport relaxation time. The other terms describe the intersubband scattering.

Equations (4)–(6) are derived with the use of the Born approximation in which the electron wave functions of the initial and final states are supposed to be plane waves in the longitudinal direction. In the frame of this approximation the density of states undergoes a steplike increase at the threshold of the topological transition $E_F=E_2$. As a result the probability of scattering $W^{(1,2)}_{\mathbf{k},\mathbf{k}'}$ in Eq. (6) also exhibits a sharp steplike increase at the threshold. Indeed, the argument of the δ function in Eq. (6) never goes to zero if $E_F<E_2$. However, it is clear that the random potential $V(\mathbf{r})$ perturbs strongly the electron states within some energy interval around the bottom of the second subband. This results in the smearing of the step in the density of states and, consequently, in the smearing

of the step in the relaxation time.

Let us denote with γ the characteristic smearing energy of the bottom of the second subband. Obviously enough, formula (7) is valid only outside this interval, i.e., for $E_F-E_2>\gamma$. Inside it, $|E_F-E_2|\leq\gamma$ the Born approximation fails. It is important to note that the electron states with energies close to E_F in the first subband are slightly affected by the random potential due to the inequality $\gamma\ll E_2-E_1$, which is usually well satisfied. The same inequality permits one to neglect the contribution to the conductivity from the electrons of the second subband in the vicinity of the transition. Really, if $|E_F-E_2|\sim\gamma$ then the concentration n_2 of the electrons in the second subband is small, $n_2/n_1\sim\gamma/(E_2-E_1)\ll 1$, while the mobilities μ_1 and μ_2 are comparable. We come to the conclusion that the states in the second subband are important only as intermediate states in the process of scattering of the electrons from the first subband.

Neglecting the term proportional to n_2 one finds from Eq. (2),

$$\sigma=\frac{n_1e^2\tau_1}{m}\ , \tag{8}$$

where

$$\tau_1^{-1}=\tau_{\rm intra}^{-1}+\tau_{\rm inter}^{-1}\ , \tag{9}$$

$$\tau_{\rm intra}^{-1}=\frac{2\pi\hbar^2}{m}\int\frac{d^2k}{(2\pi)^2}\delta(\varepsilon_1(\mathbf{k})-E_F)\times\sum_{\mathbf{k}'}W_{\mathbf{k},\mathbf{k}'}^{(1,1)}\left[1-\frac{\mathbf{k}\cdot\mathbf{k}'}{k^2}\right]\ , \tag{10}$$

$$\tau_{\rm inter}^{-1}=\frac{2\pi\hbar^2}{m}\int\frac{d^2k}{(2\pi)^2}\delta(\varepsilon_1(\mathbf{k})-E_F)\sum_{\mathbf{k}'}W_{\mathbf{k},\mathbf{k}'}^{(1,2)}\ . \tag{11}$$

Here $\tau_{\rm intra}$ is intrasubband and $\tau_{\rm inter}$ is intersubband relaxation times. Only the latter exhibits the strong variation at the threshold of the topological transition. In order to take into account the distortion of the states in the second subband by the random potential, it is convenient first to rewrite the sum in Eq. (11) in the following form:

$$\sum_{\mathbf{k}'}W_{\mathbf{k},\mathbf{k}'}^{(1,2)}=\frac{2}{\hbar}\,{\rm Im}[(1,\mathbf{k}|\langle V(\mathbf{r})G^{(2)}(\mathbf{r},\mathbf{r}')V(\mathbf{r}')\rangle|1,\mathbf{k})]\ , \tag{12}$$

where the Green function of the electron in the second subband,

$$G^{(2)}(\mathbf{r},\mathbf{r}')=\sum_{\mathbf{k}'}\frac{|2,\mathbf{k}')(2,\mathbf{k}'|}{E_F-\varepsilon_2(\mathbf{k}')}\ , \tag{13}$$

is introduced.

It can be shown that the exact [in the parameter $\gamma/(E_2-E_1)\ll 1$] expression for $\tau_{\rm inter}$ which is valid in the transitional region $|E_F-E_2|\sim\gamma$ corresponds to the replacement in Eq. (12) of the free-electron Green function (13) by the Green function in the random potential. If we present formula (12) as

$$\sum_{\mathbf{k}'}W_{\mathbf{k},\mathbf{k}'}^{(1,2)}=\frac{2}{\hbar}\,{\rm Im}\left\langle V_{12}\frac{1}{E_F-\hat{H}_2}V_{21}\right\rangle_{\mathbf{k},\mathbf{k}}\ , \tag{14}$$

where

$$\hat{H}_i=-\frac{\hbar^2}{2m}\Delta_\rho+E_i \tag{15}$$

is the Hamiltonian of the free longitudinal motion in the ith subband and the matrix elements are

$$V_{ij}(\boldsymbol{\rho})=\int_{-\infty}^{\infty}dz\,\Psi_i(z)V(\mathbf{r})\Psi_j(z)\ , \tag{16}$$

then the generalization of (14) in the transitional region implies the replacement of the operator $(E_F-\hat{H}_2)^{-1}$ by the operator $\hat{G}_{22}$ defined as

$$\hat{G}_{ij}=\int_{-\infty}^{\infty}dz\,\Psi_i(z)\frac{1}{E_F-\hat{H}-V(\mathbf{r})}\Psi_j(z)\ , \tag{17}$$

where

$$\hat{H}=-\frac{\hbar^2}{2m}\Delta_\rho-\frac{\hbar^2}{2m}\frac{\partial^2}{\partial z^2}+U(z) \tag{18}$$

is the full Hamiltonian of the electron in the 2D system. $U(z)$ is the potential confining the electron in the z direction.

Since we had restricted the consideration to the two subband approximation only the operators $\hat{G}_{ij}$ (17) with $(i,j=1,2)$ are important. Then it is easy to verify the following relations between these operators:

$$\hat{G}_{22}=\hat{G}_{22}^{(0)}+\hat{G}_{22}^{(0)}V_{22}\hat{G}_{22}+\hat{G}_{22}^{(0)}V_{21}\hat{G}_{12}\ , \tag{19}$$

$$\hat{G}_{12}=\hat{G}_{11}^{(0)}V_{11}\hat{G}_{12}+\hat{G}_{11}^{(0)}V_{12}\hat{G}_{22}\ , \tag{20}$$

where $\hat{G}_{ij}^{(0)}=(E_F-\hat{H}_i)^{-1}$. From Eqs. (19) and (20) follows the representation

$$\hat{G}_{22}=[E_F-\hat{H}_2-V_{22}-V_{21}(E_F-\hat{H}_1-V_{11})^{-1}V_{12}]^{-1}\ . \tag{21}$$

Substituting (21) instead of $(E_F-\hat{H}_2)^{-1}$ in (14) one finds

$$\sum_{\mathbf{k}'}W_{\mathbf{k},\mathbf{k}'}^{(1,2)}=-\frac{2}{\hbar}\,{\rm Im}\left\langle V_{12}\frac{1}{E_F-\hat{H}_2-V_{22}-V_{21}\dfrac{1}{E_F-\hat{H}_1-V_{11}}V_{12}}V_{21}\right\rangle_{\mathbf{k},\mathbf{k}}\ . \tag{22}$$

The term V_{11} in the denominator describes the intrasubband scattering of the electron in the first subband. The consideration given above proves that it may be neglected with the accuracy $\gamma/(E_2-E_1)$.

Expression (22) can be rewritten in a more convenient form. Note that the operator $\hat{G}_{11}$ has the representation

$$\hat{G}_{11}=[E_F-\hat{H}_1-V_{11}-V_{12}(E_F-\hat{H}_2-V_{22})^{-1}V_{21}]^{-1} \tag{23}$$

similar to (21). Let us perform the configurational averaging in (23) and introduce the self-energy part $\Sigma_1(\mathbf{k})$ according to the definition

$$\langle \hat{G}_{11} \rangle_{\mathbf{k}}=\frac{1}{E_F-\varepsilon_1(k)-\Sigma_1(\mathbf{k})} . \tag{24}$$

$\Sigma_1(\mathbf{k})$ describes both the intrasubband and the intersubband scattering processes of the electron in the first subband. If we neglect formally the term V_{11} in Eq. (23), then the intersubband processes only will contribute to the self-energy. Let us denote this part of Σ_1 as Σ_1^{inter}. Then it is easy to justify the following relation:

$$\sum_{\mathbf{k}'} W_{\mathbf{k},\mathbf{k}'}^{(1,2)}=-\frac{2}{\hbar}\,\mathrm{Im}\,\Sigma_1^{\text{inter}}(\mathbf{k}) . \tag{25}$$

Equation (25) reduces the description at the topological transition to the calculation of the self-energy part of the Green function. This calculation is carried out in the next section.

III. THE SELF-ENERGY PART CALCULATION

Let us suppose that the random potential $V(\mathbf{r})$ is Gaussian with the correlator

$$Q(\mathbf{r}-\mathbf{r}')=\langle V(\mathbf{r})V(\mathbf{r}')\rangle . \tag{26}$$

It is clear from Eqs. (23) and (24) that the perturbation theory series for the self-energy Σ_1^{inter} includes the following quantities:

$$\begin{aligned} D_{ij}^{lm}(\mathbf{k}) &= \int d^2\rho \langle V_{ij}(\boldsymbol{\rho})V_{lm}(\boldsymbol{\rho}')\rangle e^{i\mathbf{k}\cdot(\boldsymbol{\rho}-\boldsymbol{\rho}')} \\ &= \int d^2\rho \int_{-\infty}^{\infty} dz \int_{-\infty}^{\infty} dz' \Psi_i(z)\Psi_j(z)\Psi_l(z')\Psi_m(z')Q(\mathbf{r}-\mathbf{r}')e^{i\mathbf{k}\cdot(\boldsymbol{\rho}-\boldsymbol{\rho}')} . \end{aligned} \tag{27}$$

The first several terms of the diagram expansion for Σ_1^{inter} are shown in Fig. 2. In this picture the free Green functions $[E_F-\varepsilon_1(k)]^{-1}$ and $[E_F-\varepsilon_2(k)]^{-1}$ describing the electron propagation in the first and the second subbands are represented by the single and double lines, respectively. To each dashed line corresponds the correlator D_{ij}^{lm}, where i,j and l,m are the indexes of the Green functions which the dashed line separates in its beginning and in its end, respectively. Note that according to the definition of Σ_1^{inter} its diagram expansion contains no diagrams with two single lines having the common vertex since these diagrams describe the processes which include the intrasubband scattering of the electron in the first subband.

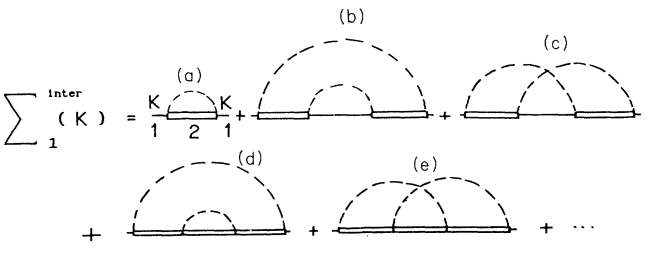

FIG. 2. First several diagrams for the self-energy part of the first subband Green function. The free Green functions of the first and second subbands are presented by the single and double lines, respectively. To each dashed line corresponds the correlator (27).

It is useful to adopt the two-step analysis of the diagram series. First let us totally neglect the intrasubband scattering of the electron in the second subband. That means that it is supposed $V_{22}\equiv 0$ in Eq. (23). Then the series in Fig. 2 includes only the diagrams (a), (b), and (c) and the other ones in which each vertex separates the single line and the double one.

Let us demonstrate that the main contribution to Σ_1^{inter} comes from the diagrams of the type shown in Fig. 3(a). Let us call this sequence of diagrams the main sequence. Each diagram of the main sequence satisfies the following rule: every single line in the diagram is covered with the dashed line which starts in the beginning and finishes in the end of the single line. It is also easy to see that any diagram satisfying this rule belongs to the main sequence.

The distinguished role of the diagrams of the main sequence is provided by the strong difference in the magnitudes of the electron momentum in the first and in the second subband. The typical value of the momentum in the first subband $P\sim[m(E_2-E_1)]^{1/2}$ is much greater than that in the second subband $q\sim(m\gamma)^{1/2}$, so that $q/P\sim[\gamma/(E_2-E_1)]^{1/2}\ll 1$.

To demonstrate that the diagrams out of the main sequence are suppressed by the factor $\gamma/(E_2-E_1)$ let us first compare two diagrams of the same order of the perturbation theory shown in Fig. 3(b). The first diagram does not belong to the main sequence while the second one does belong. The momenta along the double lines of the first diagram are $\mathbf{q}$ and $(\mathbf{K}+\mathbf{P}-\mathbf{q})$, where $\mathbf{K}$ is the incoming momentum from the first subband. Since the typ-

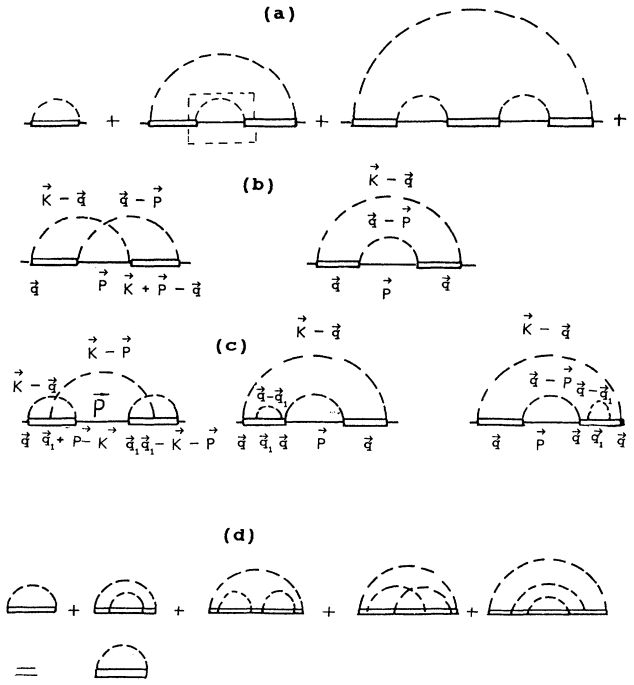

FIG. 3. (a) The main sequence of diagrams in the case $V_{22}=0$. (b) Two diagrams of the same order of the perturbation theory. The first is suppressed by the parameter $\gamma/(E_2-E_1)\ll 1$. (c) New types of diagrams appearing when the potential V_{22} is taken into account. (d) The resulting diagram series for the self-energy.

ical value of both momenta is $(m\gamma)^{1/2}$ it follows that $|\mathbf{K}+\mathbf{P}|\sim(m\gamma)^{1/2}$, while $|\mathbf{K}|\sim|\mathbf{P}|\sim[m(E_2-E_1)]^{1/2}$. For this reason the substantial contribution to the integral over d^2P gives only a small phase volume in which $\mathbf{P}$ and $\mathbf{K}$ are almost antiparallel. Such a limitation results in the fact that the first diagram is suppressed by the factor $\gamma/(E_2-E_1)$. In contrast to the first diagram the second one has no limitation on the region of integration over d^2P as it is seen from Fig. 3(b). Similar consideration can be applied for the analysis of the more complicated diagrams. If the diagram does not belong to the main sequence, then it has at least one double line with the momentum $\mathbf{q}+\mathbf{P}_1-\mathbf{P}_2$, where $|\mathbf{q}|\sim(m\gamma)^{1/2}$ and $|\mathbf{P}_1|\sim|\mathbf{P}_2|\sim[m(E_2-E_1)]^{1/2}$. Therefore there is a strong restriction $|\mathbf{P}_1-\mathbf{P}_2|\ll|\mathbf{P}_1|,|\mathbf{P}_2|$ on the region of integration over d^2P_1, d^2P_2, which makes the diagram of no importance.

The summation of the diagrams of the main sequence can be easily performed. Note that the expression for the basic fragment marked by the box in the second diagram in Fig. 3(a),

$$\int\frac{d^2P}{(2\pi)^2}\frac{D_{21}^{12}(\mathbf{P}-\mathbf{q})}{E_F-E_1-\dfrac{\hbar^2P^2}{2m}+i\delta}, \tag{28}$$

slowly varies with respect to q since $q\ll P$. Therefore one can neglect q in Eq. (28). Then the imaginary part of Eq. (28) takes the form

$$\frac{\Gamma}{2}=\pi\int\frac{d^2P}{(2\pi)^2}D_{21}^{12}(P)\delta\left[E_F-E_1-\frac{\hbar^2P^2}{2m}\right]. \tag{29}$$

The real part of Eq. (28) describes the shift of the level E_2 by the random potential. It is determined by the values of P for which the correlator $D_{21}^{12}(P)$ falls off substantially. In the further consideration we shall suppose that this shift is already included in the definition of E_2. As a result the main sequence reduces to the geometric progression. Its summation gives the following expression for $\Sigma_1^{\text{inter}}(k)$:

$$\Sigma_1^{\text{inter}}(k)=\int\frac{d^2q}{(2\pi)^2}\frac{D_{12}^{21}(\mathbf{K}-\mathbf{q})}{E_F-E_2-\dfrac{\hbar^2q^2}{2m}+\dfrac{i\Gamma}{2}}. \tag{30}$$

Taking into account that $K\gg q$ we find for the imaginary part of Eq. (30),

$$\operatorname{Im}\Sigma_1^{\text{inter}}(k)=\frac{mD_{12}^{21}(K)}{4\hbar^2}\left[1+\frac{2}{\pi}\arctan\left[2\frac{E_F-E_2}{\Gamma}\right]\right]. \tag{31}$$

Equation (31) states that if the intrasubband scattering in the second subband is neglected, the characteristic smearing energy of the bottom of the second subband equals Γ, i.e., $\gamma\sim\Gamma$.

Let us now take into account the potential V_{22} in Eq. (23) which is responsible for the intrasubband scattering in the second subband. Now the diagrams with vertices in which two double lines meet are to be considered. We start the analysis of the diagram series with the observation that the diagrams which include correlators D_{22}^{12} and D_{12}^{22} are negligible. The presence of these correlators leads to the appearance of large momentum along the double line. For example, diagram (e) in Fig. 2 appears to be negligible compared to diagram (d). Therefore from all the diagrams to which V_{22} gives rise only those including the correlator D_{22}^{22} are significant.

It is important to note that the dashed lines corresponding to the correlator D_{22}^{22} have no common vertices with the single lines. Thus the rule for the selection of the substantial diagrams formulated earlier remains in force, namely, every single line should be covered with the dashed line having the common vertices with this line. Figure 3(c) illustrates this statement. Three diagrams shown in this figure are of the same order of the perturbation theory. The first diagram does not satisfy the rule, while the second and third do satisfy it. It is seen that the violation of the rule leads to the appearance of the momenta $\mathbf{q}+\mathbf{P}-\mathbf{K}$ and $\mathbf{q}_1+\mathbf{K}-\mathbf{P}$ along the double lines and, hence, to the restriction of the region of integration over d^2P.

After the latter note the role of the diagrams with the single lines reduces to the modification of the energy E_2 in the double lines. Indeed, into each double line one, two, etc. fragments marked in Fig. 3(a) can be installed. The summation of the corresponding geometric progres-

sion, as it was demonstrated above, is equivalent to the change $E_2 \to E_2 - i\Gamma/2$ in the double line, with Γ defined by Eq. (29).

Now we are faced with the problem of the summation of all the diagrams consisting of the double lines only. Examples of these diagrams are shown in Fig. 3(d). It is seen that each diagram is covered with the common dashed line. That follows from the fact that the incoming and the outgoing momentum K is great: $K \sim [m(E_2 - E_1)]^{1/2} \gg (m\gamma)^{1/2}$. Such momentum can pass only through the dashed line. In the opposite case the appearance of the correlators D_{22}^{12}, D_{12}^{22} and, hence, the great momenta along the double lines is unavoidable.

Note now, that if we remove the covering dashed line from each diagram then the diagram series in Fig. 3(d) will be simply the averaged Green function of the electron in the second subband. As a result we come to the following formula for Σ_1^{inter}:

$$\Sigma_1^{\text{inter}}(\mathbf{k}) = \int \frac{d^2q}{(2\pi)^2} D_{12}^{21}(\mathbf{K}-\mathbf{q}) \left\langle G_{22}\left[q, E_F - E_2 + \frac{i\Gamma}{2}\right]\right\rangle . \tag{32}$$

Using the fact that $|\mathbf{K}| \gg |\mathbf{q}|$, the imaginary part of Eq. (32) can be rewritten in the form

$$\operatorname{Im}\Sigma_1^{\text{inter}}(\mathbf{k}) = D_{12}^{21}(K)\left\langle \operatorname{Im}\int \frac{d^2q}{(2\pi)^2} G_{22}\left[\mathbf{q}, E_F - E_2 + \frac{i\Gamma}{2}\right]\right\rangle = D_{12}^{21}(K)\operatorname{Im}\left\langle \sum_n \frac{1}{E_F - E_2 + \frac{i\Gamma}{2} - \varepsilon_n}\right\rangle , \tag{33}$$

where ε_n are the eigenvalues of the Hamiltonian

$$-\frac{\hbar^2}{2m}\Delta_\rho \varphi_n(\boldsymbol{\rho}) + V_{22}(\boldsymbol{\rho})\varphi_n(\boldsymbol{\rho}) = \varepsilon_n \varphi_n(\boldsymbol{\rho}) . \tag{34}$$

Introducing the density of states in the second subband

$$g_2(\varepsilon) = \left\langle \sum_n \delta(\varepsilon - \varepsilon_n)\right\rangle , \tag{35}$$

we can present the final result as

$$\begin{aligned}\operatorname{Im}\Sigma_1^{\text{inter}}(\mathbf{k}) &= D_{12}^{21}(K)\operatorname{Im}\left\langle \int_{-\infty}^{\infty} d\varepsilon \frac{1}{E_F - E_2 + i\Gamma/2 - \varepsilon} \sum_n \delta(\varepsilon - \varepsilon_n)\right\rangle \\ &= \frac{D_{12}^{21}(K)\Gamma}{2}\int_{-\infty}^{\infty} d\varepsilon \frac{d\varepsilon\, g_2(\varepsilon)}{(E_F - E_2 - \varepsilon)^2 + \frac{\Gamma^2}{4}} .\end{aligned} \tag{36}$$

Formula (36) is the basic result of this section. It is easy to see that for $V_{22} \equiv 0$ and

$$g_2(\varepsilon) = g_2^{(0)}(\varepsilon) = \frac{m}{2\pi\hbar^2}\Theta(\varepsilon) , \tag{37}$$

$\Theta(\varepsilon)$ being the unit-step function, Eq. (36) reduces to Eq. (31)

IV. THE CONDUCTIVITY AND THERMOPOWER IN THE VICINITY OF THE TRANSITION

The expression for the intersubband relaxation time can now be easily found by substituting Eqs. (36) and (25) in Eq. (11) and using Eq. (29),

$$\frac{1}{\tau_{\text{inter}}} = \frac{\hbar\Gamma^2}{m}\int_{-\infty}^{\infty} d\varepsilon \frac{g_2(\varepsilon)}{(E_F - E_2 - \varepsilon)^2 + \frac{\Gamma^2}{4}} . \tag{38}$$

This expression is the main result of the paper. It describes the peculiarity in the behavior of the conductivity in the vicinity of the topological transition. Using the conventional relation between the conductivity and thermopower,

$$\alpha = \frac{\pi^2 T}{3e}\frac{\partial \ln\sigma}{\partial E_F} = \frac{\pi^2 T}{3e}\tau_1 \frac{\partial}{\partial E_F}\left[\frac{1}{\tau_{\text{inter}}}\right] , \tag{39}$$

and substituting Eq. (38) in Eq. (39), we get

$$\alpha = \frac{\pi^2}{3}\frac{\hbar T\Gamma^2\tau_1}{em}\int_{-\infty}^{\infty} d\varepsilon \frac{\partial g_2(\varepsilon)/\partial\varepsilon}{(E_F - E_2 - \varepsilon)^2 + \frac{\Gamma^2}{4}} . \tag{40}$$

Here T is the temperature and τ_1 is the total relaxation time (9). In Eq. (39) it is taken into account that only τ_{inter} exhibits the sharp variation in the vicinity of the transition.

Further calculations are possible only if we specify the properties of the random potential. We shall consider two typical examples. The first is the potential, created by the randomly distributed short-range impurities ("white noise"). The second is the potential of the Coulomb centers.

A. White-noise potential

In this case the correlator (26) is known to be

$$Q(\mathbf{r}-\mathbf{r}')=C\delta(\mathbf{r}-\mathbf{r}') \tag{41}$$

and therefore the quantities D_{ij}^{lm},

$$D_{ij}^{lm}=C\int_{-\infty}^{\infty} dz\ \Psi_i(z)\Psi_j(z)\Psi_l(z)\Psi_m(z)\ , \tag{42}$$

do not depend on K. The width Γ according to the definition (29) equals

$$\Gamma=\frac{m}{\hbar^2}D_{12}^{21}=\frac{mC}{\hbar^2}\int_{-\infty}^{\infty} dz\ \Psi_1^2(z)\Psi_2^2(z)\ . \tag{43}$$

The 2D density of states in the white-noise potential was studied in Refs. 11 and 12. It is convenient to present it in the following form:

$$g_2(\varepsilon)=\frac{m}{2\pi\hbar^2}f\left[\frac{\varepsilon}{E_0}\right]\ , \tag{44}$$

where E_0 is the characteristic energy scale,

$$E_0=\frac{m}{\hbar^2}D_{22}^{22}=\frac{mC}{\hbar^2}\int_{-\infty}^{\infty} dz\ \Psi_2^4(z)\ , \tag{45}$$

and f is the dimensionless function which has the following asymptotic behavior:

$$f(x)=\begin{cases}1-\dfrac{1}{2\pi x}, & x\gg 1\\ 0.314|x|^{0.57}\exp(-5.84|x|)\ , & x<0 \text{ and } |x|\gg 1\ .\end{cases} \tag{46}$$

It is clear from (43) and (45) that the quantities Γ and E_0 are comparable.

In order to present the results of the numerical calculations of τ_{inter} it is convenient to rewrite Eq. (38) using Eq. (44) in the form

$$\tau_{\text{inter}}^{-1}=\frac{\Gamma}{\hbar}F_\tau\left[\frac{2(E_F-E_2)}{\Gamma},\nu\right]\ , \tag{47}$$

where

$$\nu=\frac{\Gamma}{2E_0} \tag{48}$$

and the function F_τ is defined as

$$F_\tau(Y,\nu)=\frac{1}{\pi}\int_{-\infty}^{\infty} dt\frac{f(\nu t)}{(Y-t)^2+1}\ . \tag{49}$$

The plots of F_τ calculated for various ν are presented in Fig. 4(a). Its argument $Y=2(E_F-E_2)/\Gamma$ characterizes the proximity to the transition. In calculations the function f presented in Ref. 11 was used. It is seen from Fig. 4(a) that the interval of E_F in which τ_{inter}^{-1} and, hence, the conductivity exhibits the sharp variation is determined by the higher energy Γ or E_0, i.e., $\gamma\simeq\max\{\Gamma,E_0\}$.

The expression for the thermopower after substitution of (44) in (40) takes the form

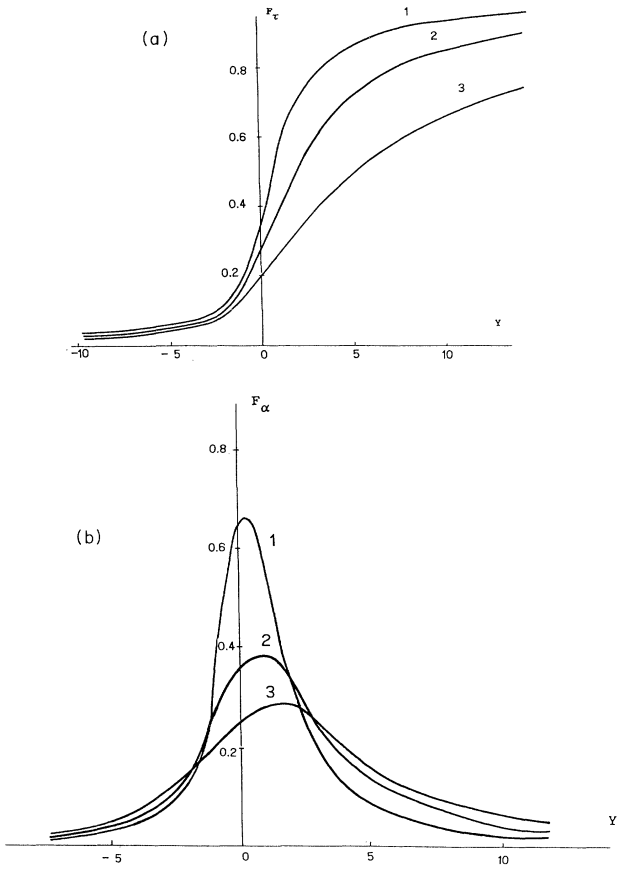

FIG. 4. The normalized inverse intersubband relaxation time (a) and thermopower (b) as the functions of the Fermi-level position $[Y=2(E_F-E_2)/\Gamma]$ in the case of the "white-noise" random potential. Curves 1,2,3 correspond to $\nu=\Gamma/2E_0=0.3,1,3$, respectively.

$$\alpha=\alpha_0 F_\alpha(Y,\nu)\ , \tag{50}$$

where

$$\alpha_0=\frac{2\pi T\tau_1}{3e\hbar} \tag{51}$$

and

$$F_\alpha(Y,\nu)=\nu\int_{-\infty}^{\infty} dt\frac{f'(\nu t)}{(Y-t)^2+1}\ . \tag{52}$$

Figure 4(b) shows the behavior of F_α vs Y for various ν. It is seen that the peak of thermopower in the vicinity of the transition has an asymmetrical form. This asymmetry is the most important qualitative result of the present paper. It is the consequence of the behavior of the 2D density of states in the white-noise potential. Indeed, for $E_0\to 0$, i.e., $\nu\to\infty$, we obtain from Eq. (52) the symmetrical Lorentzian peak in thermopower,

$$F_\alpha(Y,\infty)=\frac{\Gamma^2}{4(E_F-E_2)^2+\Gamma^2}\ . \tag{53}$$

Note that in the previous works[9,13] in which the con-

ductivity in the vicinity of the transition was considered, the smearing of the density of states in the second subband was neglected. Therefore the approach of Refs. 9 and 13 leads to the symmetrical peak (53) in thermopower at low temperatures (see Ref. 14). That contradicts our prediction, since, as it was shown above, $E_0 \sim \Gamma$.

It is significant to emphasize the difference between the 2D case considered and the 3D case. In 3D the unperturbed density of states $g(\varepsilon) \propto \varepsilon^{1/2}$ results in the asymmetry of thermopower.[6] The smearing E_0 of density of states in 3D is negligible. The reason for this is that E_0 in 3D is proportional to the second power of the random potential correlator (41), $E_0 \propto C^2$ (see Ref. 15), in contrast to $\Gamma \sim C$. Therefore the inequality $E_0 \ll \Gamma$ holds in 3D. In 2D we have $E_0 \sim \Gamma$ and the only source of the asymmetry is the smearing of the density of states.

B. Coulomb potential

Let us suppose that the random potential $V(\mathbf{r})$ is created by the charged donors providing the conduction channel with the electrons. The electron gas screens the Coulomb potential of each donor. The typical space scale of the resulting effective potential is of the order of the screening radius. The latter is known to be about the Bohr radius $a_B = \hbar^2\kappa/me^2$ (here κ is the dielectric constant) in the 2D case.[10] Under the condition $E_2 - E_1 \gg \hbar^2/ma_B^2$, which is normally met, the de Broglie wavelength of the electron in the first subband $\hbar/[2m(E_2 - E_1)]^{1/2}$ is much less than the screening radius. That means that the potential $V(\mathbf{r})$ affecting the electrons can be considered as quasiclassical and characterized by the distribution function[16]

$$\xi(V) = \frac{1}{\pi^{1/2} W} \exp\left[-\frac{V^2}{W^2} \right] , \tag{54}$$

where

$$W = \langle 2V^2 \rangle^{1/2} \tag{55}$$

is the mean square root potential. The validity of quasiclassical treatment permits us also to suppose the bottom of the second subband to be shifted smoothly by the potential $V(\mathbf{r})$ in each point $\mathbf{r}$. Then the density of states is given by the expression[16]

$$g_2(\varepsilon) = \int_{-\infty}^{\infty} dV\, \xi(V) g_2^{(0)}(\varepsilon - V) , \tag{56}$$

where $g_2^{(0)}$ is the unperturbed density of states (37). The integral (56) is the known error function

$$g_2(\varepsilon) = \frac{m}{2\pi\hbar^2} \Phi(\varepsilon/W) , \tag{57}$$

$$\Phi(x) = \frac{1}{\pi^{1/2}} \int_{-\infty}^{x} dt \exp(-t^2) . \tag{58}$$

Comparing (44) with (57) we find the expressions for τ_{inter} and α in the form (47) and (50) with the replacement of the functions F_τ and F_α by

$$\tilde{F}_\tau(Y,\tilde{\nu}) = \frac{1}{\pi} \int_{-\infty}^{\infty} dt \frac{\Phi(\tilde{\nu}t)}{(Y-t)^2+1} , \tag{59}$$

$$\tilde{F}_\alpha(Y,\tilde{\nu}) = \tilde{\nu} \int_{-\infty}^{\infty} dt \frac{\Phi'(\tilde{\nu}t)}{(Y-t)^2+1} , \tag{60}$$

where

$$\tilde{\nu} = \frac{\Gamma}{2W} . \tag{61}$$

The behavior of the functions $\tilde{F}$ and $\tilde{F}$ vs $Y = 2(E_F - E_{2)}/\Gamma$ for various $\tilde{\nu}$ is shown in Fig. 5. The thermopower is now a symmetrical function of Y. This is the consequence of the following property of the 2D density of states (57) in a smooth potential:

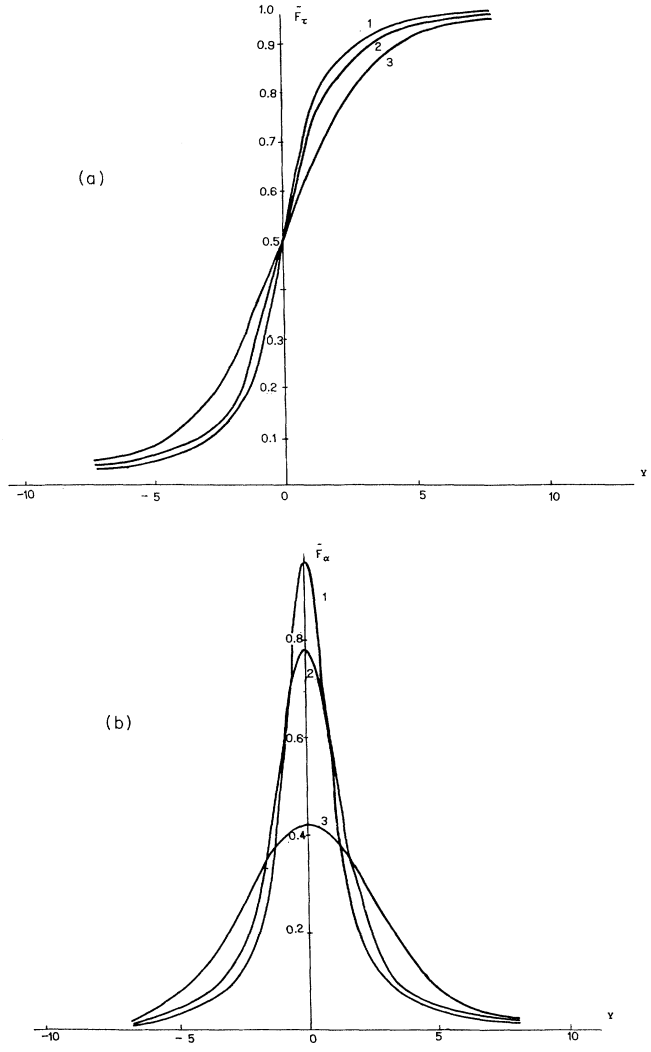

FIG. 5 The normalized inverse intersubband relaxation time (a) and thermopower (b) as the functions of the Fermi-level position $[Y = 2(E_F - E_2)/\Gamma]$ is the case of the random potential produced by the charged donors. Curves 1,2,3 correspond to $\tilde{\nu} = \Gamma/2W = 0.3, 1, 3$, respectively.

$$g_2(\varepsilon)+g_2(-\varepsilon)=\frac{m}{2\pi\hbar^2} . \tag{62}$$

The relation between Γ and W depends strongly on the location of donors in space. We consider the typical case when the donors are arranged in a plane removed by the distance z_0 (the thickness of the spacer layer) from the conducting channel. Using the results of Ref. 10 the quantities D_{ij}^{lm} (27) can be presented in this case as

$$D_{ij}^{lm}(k)=\left[\frac{2\pi e^2}{\kappa}\right]^2 \frac{Ne^{-2kz_0}}{\left[k+\frac{2}{a_B}\right]^2}\mathcal{J}_{ij}(k)\mathcal{J}_{lm}(k) , \tag{63}$$

where N is the 2D concentration of donors, the form factors $\mathcal{J}_{ij}$ are

$$\mathcal{J}_{ij}(k)=\int_0^\infty dz\, \Psi_i(z)\Psi_j(z)e^{-kz} \tag{64}$$

($z=0$ is the boundary of the conducting channel). Using expressions (27) and (55) the smearing of the second subband W can be written in the form

$$W^2=2\int \frac{d^2k}{(2\pi)^2}D_{22}^{22}(k) . \tag{65}$$

Substituting (63) in (65) we obtain

$$W^2=16\pi(Na_B^2)E_B^2\int_0^\infty dt\frac{te^{-4tz_0/a_B}}{(t+1)^2}\mathcal{J}_{22}^2\left[\frac{2t}{a_B}\right] , \tag{66}$$

where $E_B=\hbar^2/2ma_B^2$ is the Bohr energy.

The expression for Γ can be obtained by substituting (63) in (29) and taking into account that the Fermi momentum in the first subband,

$$K_0=\frac{[2m(E_2-E_1)]^{1/2}}{\hbar} , \tag{67}$$

is large, $K_0\gg 1/a_B$. Then we have

$$\Gamma=\frac{8\pi^2(Na_B^2)E_B^2}{E_2-E_1}\mathcal{J}_{21}^2(K_0)\exp(-2K_0z_0) . \tag{68}$$

It is clear from (66) and (68) that the dependence of Γ and W on the thickness of the spacer z_0 is substantially different. If $z_0>1/K_0$, then Γ exponentially decreases with the increase of z_0 and we have $\Gamma\ll W$. Therefore the approach of Refs. 9 and 13 in which W was neglected proves to be inadequate.

In the region $z_0\leq 1/K_0$ an *a priori* statement about the ratio Γ/W is impossible. The parameter Na_B^2 usually is of order of unity and the form factors $\mathcal{J}_{22}$ and $\mathcal{J}_{12}$ which do depend on the wave functions $\Psi_1(z)$ and $\Psi_2(z)$ play the decisive role.

Note in conclusion of this section that the derivation of (63) is based on the fact that the screening is fulfilled by the electrons of the first subband only, but with the increase of E_F the electrons of the second subband also take part in screening. As a result the screening radius diminishes. This effect causes the slight asymmetry of the thermopower peak. It falls off more rapidly towards high E_F in contrast to the case of the white-noise random potential.

V. CONCLUSION

In the present paper the behavior of the conductivity and thermopower of a 2D electron gas in the case when the Fermi level crosses the next size-quantization level is studied. The sensitivity of these quantities to the position of the Fermi level around the bottom of a new subband is caused by the processes of intersubband scattering of the electrons from the populated subband. It is shown that there are two reasons and, consequently, two parameters that determine the rounding of the discontinuity in the Fermi-level dependence of the conductivity predicted by the Boltzmann equation in the vicinity of the transition. First is the finite lifetime $\hbar/\Gamma$ of the electronic states in the populating subband, caused by the possibility of their elastic scattering into the states of the lower subbands. Second is the smearing E_0 or W of the density of states in the populating subband, caused by the random potential. It is important that in the 2D case both parameters are, in principle, of the same order $\Gamma\sim E_0$ or $\Gamma\sim W$. On the contrary, in 3D we have E_0, $W\ll\Gamma$, and only the lifetime broadening Γ of the populating states is significant.

Note that in the transitional region $|E_F-E_i|\sim\gamma=\max\{\Gamma,E_0\}$ the structure of the 2D wave functions of the electronic states in a newly populating subband is very complicated. Just in this region the localization threshold for these states is situated. However in the calculation of the conductivity and thermopower such a complicated structure of the wave functions appears to be of no importance. The reason for this is the strong difference in the space scales of the wave functions in newly populating and in lower subbands. The de Broglie wavelength of the electron in the lower subband is much less than $\hbar/(m\gamma)^{1/2}$—the typical size of the wave function in the new subband. As it was mentioned above, the states in the new subband act exclusively as the intermediate states in the scattering processes of the electrons from the lower subbands. Then the electron with the small wavelength, being scattered into such a "wide" state, does not "feel" the complicated arrangement of its wave function. Therefore, only the density of states in the population subband appears to be significant.

The most important qualitative result of the present research is the asymmetry of the peak in the dependence of the thermopower on the Fermi-level position in case of the white-noise potential. In case of the Coulomb potential the very strong dependence of the amplitude and the width of the peak on the thickness of the spacer layer is predicted.

We had restricted our consideration to low temperatures. Note that the temperature itself may cause the rounding of the anomalies.[17] Therefore the condition for

the validity of the theory developed is $T \ll \gamma$. The treatment of the experimental data[18] based on the temperature smearing of the anomalies was carried out in Ref. 19. Besides, with the increase of temperature the effect of the phonon drag on the thermopower may become significant.[20]

ACKNOWLEDGMENTS

We are grateful to A. A. Varlamov, M. I. Dyakonov, and R. A. Suris for interesting discussions. One of the authors (M.E.R.) is grateful to the Alexander von Humboldt Foundation for support.

[1]H. L. Störmer, A. C. Gossard, and W. Wiegmann, Solid State Commun. **41**, 707 (1982).
[2]J. J. Harris, D. E. Lacklison, C. T. Foxon, F. M. Selten, A. M. Suckling, R. J. Nicholas, and K. W. J. Barnham, Semicond. Sci. Technol. **2**, 783 (1987).
[3]I. M. Lifshitz, Zh. Eksp. Teor. Fiz. **33**, 1569 (1960) [Sov. Phys. JETP **11**, 1130 (1969)].
[4]A. A. Varlamov and A. V. Pantsulaya, Zh. Eksp. Teor. Fiz. **89**, 2188 (1985) [Sov. Phys. JETP **62**, 1263 (1985)].
[5]A. A. Varlamov and A. V. Pantsulaya, Solid State Commun. **56**, 787 (1985).
[6]A. A. Varlamov and A. V. Pantsulaya, Adv. Phys. **38**, 469 (1989).
[7]E. D. Siggia and P. C. Kwok, Phys. Rev. B **2**, 1024 (1970).
[8]S. Mori and T. Ando, Phys. Rev. B **19**, 6433 (1979).
[9]D. G. Cantrell and P. N. Butcher, J. Phys. C **18**, 5111 (1985).
[10]T. Ando, A. B. Fowler, and F. Stern. Rev. Mod. Phys. **54**, 437 (1982).
[11]D. J. Thouless and M. E. Elzain, J. Phys. C **11**, 3425 (1978).
[12]E. Brezin and G. Parisi, J. Phys. C **13**, L307 (1980).
[13]W. Walukiewicz, H. E. Ruda, J. Lagowski, and H. C. Gatos, Phys. Rev. B **30**, 4571 (1984).
[14]D. G. Cantrell and P. N. Butcher, J. Phys. C **18**, 6639 (1985).
[15]A. L. Efros and M. E. Raikh, in *Optical Properties of Mixed Crystals,* edited by R. J. Eliott and I. P. Ipatova (North-Holland, Amsterdam, 1988), p. 133.
[16]B. I. Shklovskii and A. L. Efros, *Electronic Properties of Doped Semiconductors,* Springer Series in Solid State Sciences Vol. 45 (Springer, Berlin, 1984).
[17]D. G. Cantrell and P. N. Butcher, J. Phys. C **18**, L587 (1985).
[18]J. S. Davidson, E. Dan Dahlberg, A. G. Valois, and G. Y. Robinson, Phys. Rev. B **33**, 8238 (1986).
[19]D. G. Cantrell J. Phys. C **19**, L817 (1986).
[20]D. G. Cantrell and P. N. Butcher, J. Phys. C **19**, L429 (1986).